ChemPubSoc Europe

DOI: 10.1002/open.201700168

Open Access ChemistryOPEN Full Papers

Organometallic Nucleosides: Synthesis and Biological Evaluation of Substituted Dicobalt Hexacarbonyl 2′-Deoxy-5-oxopropynyluridines

Renata Kaczmarek,[a] Dariusz Korczyński,[a] Karolina Królewska-Golińska,[a] Kraig A. Wheeler,[b] Ferman A. Chavez,[c] Agnieszka Mikus,[c] and Roman Dembinski*[a, c]

Reactions of dicobalt octacarbonyl [$Co_2(CO)_8$] with 2′-deoxy-5-oxopropynyluridines and related compounds gave dicobalt hexacarbonyl nucleoside complexes (83–31 %). The synthetic outcomes were confirmed by X-ray structure determination of dicobalt hexacarbonyl 2′-deoxy-5-(4-hydroxybut-1-yn-1-yl)uridine, which exhibits intermolecular hydrogen bonding between a modified base and ribose. The electronic structure of this compound was characterized by the DFT calculations. The growth inhibition of HeLa and K562 cancer cell lines by organometallic nucleosides was examined and compared to that by alkynyl nucleoside precursors. Coordination of the dicobalt carbonyl moiety to the 2′-deoxy-5-alkynyluridines led to a significant increase in the cytotoxic potency. The cobalt compounds displayed antiproliferative activities with median inhibitory values (IC_{50}) in the range of 20 to 80 μM for the HeLa cell line and 18 to 30 μM for the K562 cell line. Coordination of an acetyl-substituted cobalt nucleoside was expanded by using the 1,1-bis(diphenylphosphino)methane (dppm) ligand, which exhibited cytotoxicity at comparable levels. The formation of reactive oxygen species in the presence of cobalt compounds was determined in K562 cells. The results indicate that the mechanism of action for most antiproliferative cobalt compounds may be related to the induction of oxidative stress.

1. Introduction

Nucleoside analogues are molecules of high pharmacological interest for the treatment of various conditions, especially cancer and viral diseases.[1–4] These agents behave as antimetabolites and compete with physiologic nucleosides, and consequently, they interact with a large number of intracellular targets to induce cytotoxicity. Substitution at the C-5 position of the uracil base provides a common framework for potent biological properties.[5]

In parallel, bioorganometallic chemistry provides new tools to influence biological interactions.[6–13] Among a variety of organometallic compounds, transition-metal carbonyls forged their presence in medicinal chemistry.[14] For example, a ruthenium carbonyl complex, a protein kinase inhibitor, activates p53 and induces apoptosis in human melanoma cells.[15] Related complexes were designed distinctly: as tamoxifen-based anticancer drug derivatives,[16,17] as inhibitors of human carbonic anhydrase (hCA),[18] as antibacterial agents,[19] and as triazoles displaying antitrypanosomal activity.[20] Representative nucleoside-related examples include rhenium tricarbonyl complexes such as **1** (Figure 1)[21] and manganese and chromium tricar-

[a] Dr. R. Kaczmarek, D. Korczyński, Dr. K. Królewska-Golińska, Prof. Dr. R. Dembinski
Department of Bioorganic Chemistry
Centre of Molecular and Macromolecular Studies
Polish Academy of Sciences, Sienkiewicza 112, 90–363 Łódź (Poland)

[b] Prof. Dr. K. A. Wheeler
Department of Chemistry, Whitworth University
300 W. Hawthorne Rd., Spokane, WA 99251 (USA)

[c] Prof. Dr. F. A. Chavez, Dr. A. Mikus, Prof. Dr. R. Dembinski
Department of Chemistry, Oakland University
146 Library Drive, Rochester, MI 48309-4479 (USA)
E-mail: dembinsk@oakland.edu

Supporting Information for this article can be found under: https://doi.org/10.1002/open.201700168.

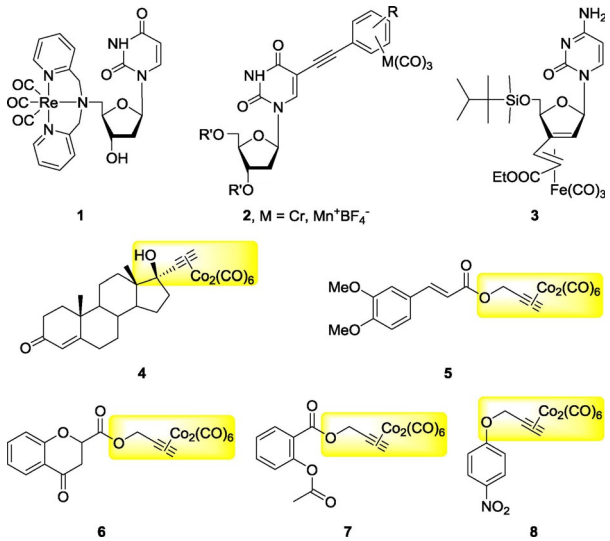

Figure 1. Structures of representative metal–carbonyl complexes with medicinal potential.

bonyl arylalkynyl nucleosides **2** (Figure 1).[22] Nucleoside–iron carbonyl complex **3** (Figure 1) was reported to bestow significant apoptosis-inducing activity against BJAB tumor cells[23] and specific cytotoxicity to reactive oxygen species (ROS)-stressed cancer cells.[24]

Cobalt possesses a diverse array of properties that can be manipulated to yield promising drug candidates.[25] The medicinal potential of cobalt carbonyl complexes has been reported.[26] Peptide labeling by using a dicobalt hexacarbonyl alkynyl complex[27] and cobalt carbonyl complexes encapsulated in a micelle structure (not illustrated), aiming to deliver cobalt pharmaceuticals,[28] has been investigated. The activity of a cobalt derivative of 17-ethynyltestosterone (**4**; Figure 1) has also been explored.[29] Recently, two cobalt-based hybrid molecules that combine an Nrf2 (a basic leucine zipper protein) inducer with a releaser of carbon monoxide (an anti-inflammatory product of heme oxygenase-1) were reported to increase Nrf2/H-O1 expression markedly and to exert anti-inflammatory activity in vitro. Compounds **5** and **6** (Figure 1) also up-regulate tissue heme oxygenase-1 and deliver CO to the blood after administration in vivo, which supports their potential anti-inflammatory properties.[30]

The antiproliferative properties of dicobalt hexacarbonyl complexes have been noted,[31–35] and aspirin–cobalt carbonyl derivative **7** containing a propargyl alcohol unit (Figure 1) was identified as a lead compound during in vitro studies against MCF-7 and MDA-MB-231 human mammary breast cancer cells.[33] Additional studies have suggested a mode of action in which cyclooxygenase inhibition plays a major role.[34] The aspirin–cobalt carbonyl derivative also exhibited antiangiogenic effects in a zebrafish embryo assay, as well as significant inhibition of matrix metalloproteinase-7 (MMP-7).[36] Among its many other demonstrated biological effects was a strong induction of caspase-3, which is an important activator in apoptosis. A related aromatic compound with a nitro substituent, that is, **8** (Figure 1), was shown to strongly induce apoptosis, arrest the cell cycle at the S phase, increase cellular oxidative stress levels, and induce permeability of the mitochondrial membrane.[37] Whereas its non-cobalt-containing precursor also caused an increase in mitochondrial membrane permeability, it did not produce an increase in oxidative stress levels, nor did it have apoptosis-inducing or antiproliferative effects.

A review of structures **4**–**8** (Figure 1) revealed a common cobalt carbonyl propargyloxy ligand (–C≡CCH$_2$O–), which appears in the form of its ester or free alcohol. Thus, we were intrigued as to whether the combination of a nucleoside with the presence of a propargyloxy structural motif would increase the potency of such conjugates. Consequently, the design of the investigated compounds included several propynoxy (propargyloxy) and related units, as discussed below.

Despite numerous advances, the repertoire of metallonucleosides is still limited. Interest in the use of the ethynyl (acetylenic) fragment for the modification of nucleoside bases has resulted in a great number of applications.[5] Our earlier studies confirmed activity against MCF-7 and MDA-MB-231 human mammary breast cancer cells of alkyl- and aryl-substituted cobalt hexacarbonyl nucleosides,[38] as well as their precursors, 5-alkynyl uridines.[39] We were intrigued to investigate further 2′-deoxy-5-alkynyluridines and their hexacarbonyl dicobalt adducts in particular to pursue the synthesis and biological evaluation of a combination of oxopropynyl (oxopropargyl), cobalt carbonyl, and nucleoside structural features as new target compounds. Enhancement of action through installment of the acetyl group was also explored.

2. Results and Discussion

2′-Deoxy-5-alkynyluridines **9a**–**h** (Scheme 1), containing a conjugated alkyne function, represent versatile materials for reactions that lead, among others, to furopyrimidines,[40] halofuropyrimidines,[41] and alkynyl dimers.[42]

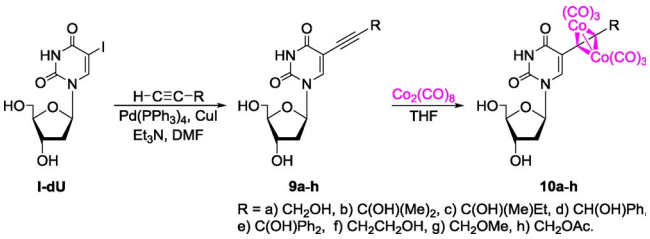

Scheme 1. Synthesis of 2′-deoxy-5-alkynyluridines **9a**–**h** from 2′-deoxy-5-iodouridine (**I-dU**).

Sonogashira coupling of alkynes offers an atom-efficient pathway toward modification of nucleosides.[39,43] Preparative synthesis of a series of 2′-deoxy-5-alkynyluridines **9** was performed from 2′-deoxy-5-iodouridine (**I-dU**) and the appropriate terminal alkyne in the presence of catalytic amounts of Pd(PPh$_3$)$_4$, copper(I) iodide, and triethylamine in DMF in a tightly controlled temperature regime (40 °C, oil bath, 22 h; Scheme 1) to avoid subsequent cyclization to furopyrimidines; this protocol did not require protection of the hydroxy groups.[39] To explore the structure–reactivity relationship of the alkyne substituents, nucleosides containing a oxopropynyl (oxypropargyl) unit (propargyl alcohol, **9a**, R = CH$_2$OH), alkyl disubstituted [**9b**/**9c**, R = C(OH)(Me)$_2$/C(OH)(Me)Et], aryl mono- and disubstituted [**9d**/**9e**, R = CH(OH)Ph/C(OH)Ph$_2$], as well as the one-carbon-extended homologue (**9f**, R = CH$_2$CH$_2$OH), methyl ether (**9g**, R = CH$_2$OMe), and acetate (**9h**, R = CH$_2$OAc) groups, were obtained in 92–41 % yield by using literature procedures (Table 1). Numerous 2′-deoxy-5-alkynyluridines have

Table 1. Preparation of 2′-deoxy-5-alkynyluridines **9a**–**h** and conversion into hexacarbonyl dicobalt derivatives **10a**–**h**.

R	Alkynyl uridine **9**	Yield [%]	Cobalt complex **10**	Yield [%]
CH$_2$OH	**9a**	50	**10a**	58
C(OH)Me$_2$	**9b**	41	**10b**	31
C(OH)(Me)Et	**9c**	56	**10c**	64
CH(OH)Ph	**9d**	46	**10d**	71
C(OH)Ph$_2$	**9e**	92	**10e**	62
CH$_2$CH$_2$OH	**9f**	54	**10f**	54
CH$_2$OMe	**9g**[44]	69	**10g**	83
CH$_2$OAc	**9h**	66	**10h**	83

been synthesized because of their interesting biological activity. However compounds **9a–f** and **9h**, to our knowledge, have not yet been reported.[44] The structures of alkynyl nucleosides **9** were confirmed by ^{1}H NMR and ^{13}C NMR spectroscopy. The high-resolution mass spectra of **9a–h** exhibit *m/z* signals of $[M+H]^+$ as molecular ions.

The conversion of alkynyl nucleosides **9** into **10**, which are the corresponding dicobalt hexacarbonyl complexes of the 2′-deoxy-5-alkynyluridines, was accomplished at room temperature [$Co_2(CO)_8$, 22 °C, 1 h], and these compounds were obtained in 83–31 % yield after silica gel column chromatography (Scheme 1, Table 1).

The structures of new nucleosides **10a–h** were confirmed by NMR and IR spectroscopy and HRMS. In most cases, the ^{1}H NMR spectra exhibit one signal in the region of H6, as expected (δ = 8.35–8.11 ppm). However, two signals are observed for compounds **10c** and **10d** (δ = 8.30/8.27 and 8.17/8.11 ppm, respectively), presumably due to the epimers at the stereocenter located at the propargyl carbon atom. It can be assumed that most molecules, due to steric reasons, would exist in solution in the conformation that resembles the one observed in the crystal structure of **10f**. This includes the planar assembly of C6–C5–C7–C8–C9, leading to potential hydrogen-bonding engagement of the propargyl and H-O5′ hydroxy groups, which would lead to restricted rotation across the C8–C9 bond. Under such circumstances, H6 would be positioned *gauche* to the hydroxy group and one of the substituents of the stereocenter, which would lead to nonmagnetically equivalent environments for each of the propargyl (C9) epimers. The H6 signals for **10c**/**10d** are separated by 21.4/30.9 Hz, respectively, in line with the anticipated lower magnetic impact of the alkyl group versus the phenyl group. The variable-temperature ^{1}H NMR spectra show significant line broadening at 60 °C, but incomplete coalescence ($CDCl_3$; higher temperature leads to decomposition). The reformation of well-separated signals is observed upon returning to 20 °C. In the ^{13}C NMR spectrum, nonequivalency of the cobalt carbonyl signals (CoCO) is observed only for **10d** (δ = 199.45 and 198.93 ppm). The IR spectra exhibit characteristic bands for the alkyne [$Co_2(CO)_6$] group [$\tilde{\nu}$ around 2092 (m), 2052 (s), and 2016 cm^{-1} (vs)]. Selected representative compounds as well as their alkynyl counterparts (i.e. compounds **9a**/**10a**, **9g**/**10g**, and **9h**/**10h**) gave acceptable elemental analyses. The high-resolution mass spectra exhibit *m/z* signal of ions $[M-OH]^+$ for **10a–f** and **10g** and $[M-OAc]^+$ for **10h**, which are presumably formed due to a dehydration or deacylation reaction during acquisition; the ability of the dicobalt hexacarbonyl moiety to stabilize a positive charge at an adjacent carbon atom is well known. Nucleoside **10f** containing a homopropargyl group, which lacks an option to form a well-stabilized carbocation, shows the *m/z* $[M+H]^+$ signal for the molecular ion.

Efforts to obtain diffraction-quality crystals were so far only successful in the case of **10f** by diffusion of pentane into a THF solution (−20 °C) under a dry nitrogen atmosphere. X-ray crystallography confirms the structure of dicobalt hexacarbonyl 2′-deoxy-5-(4-hydroxybut-1-yn-1-yl)uridine (**10f**). Although nucleosides are often resistant to crystallization, intramolecular hydrogen bonding O10···H-O5′ forms a 14-membered ring that rigidifies the structure and presumably facilitates formation of the X-ray-quality crystals (Figure 2).[45] Coordination of the alkyne to the dicobalt changes the position of the CH_2CH_2OH group relative to the pyrimidine base through the C–C≡C–C planar unit of the cobalt complex with angles of 142–143°. The R group is directed towards the ribose unit and is long enough to create a contact of O10 with the hydrogen atom of the 5′-hydroxy group O10···H-O5′ 2.809(7) Å [calcd 2.756 Å].[46]

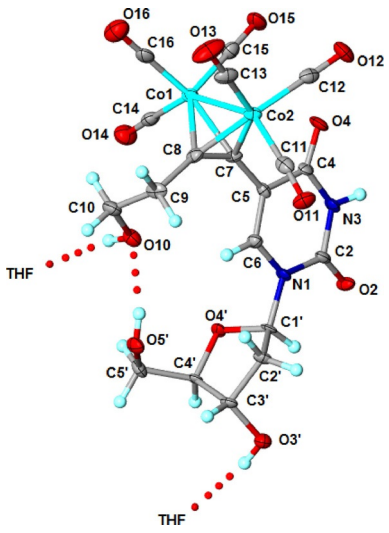

Figure 2. ORTEP view of **10f** with the atom-labeling scheme. Thermal ellipsoids are drawn at the 50 % probability level. Selected interatomic distances [Å] (calcd values are given in square brackets): C5–C7 1.452(10) [1.442], C7–C8 1.333(9) [1.359], C8–C9 1.520(9) [1.490], Co1–Co2 2.4758(16) [2.404], O10···H-O5′ 2.809(7) [2.756]; key angles [°]: C5–C7–C8 142.9(7) [140.937], C7–C8–C9 142.1(7) [141.257].

In the crystalline form, the hydrogen atoms of the remaining hydroxy groups (H-O3′ and CH_2CH_2OH) are each stabilized by a molecule of THF (O3′···O17 2.791 Å, calcd 2.754 Å; O18···O10 2.750 Å; O18A···O10 2.703 Å, calcd 2.693 Å). The C2 carbonyl group of **10f** adopts an *anti* orientation towards the ribose ring: the glycosidic bond torsion angle χ (O4′–C1′–N1–C2) is 108.3(6)°. The Co–Co bond is perpendicular to the uracil plane, and the dicobalt carbonyl unit is located *syn* to the ribose ring.

2.1. Computational Studies

DFT calculations were conducted on **10f** in the gas phase to optimize the ground-state structure.[47] The energies were acquired by using PBE0/6-31G*. Selected calculated metric parameters for the geometry-optimized structure were compared to the experimental results (Figure 2). The largest difference between the experimental and calculated bond lengths was 0.07 Å (Co1–Co2), whereas the bond angles were in good agreement. Despite slight differences, the calculated structure is quite close to the experimental structure (even reproducing hydrogen bonds), allowing electronic properties to be confidently extracted. The calculated Mulliken charge value for Co1 and Co2 in **10f** is −0.08, consistent with neutrality. Figure 3 il-

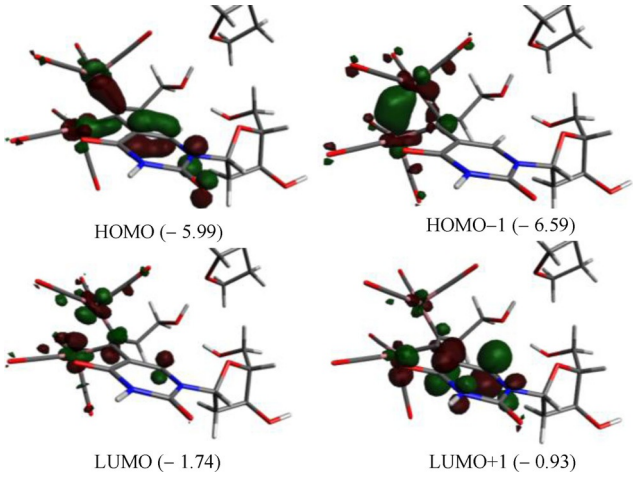

Figure 3. Plots of molecular orbitals: HOMO−1, HOMO, LUMO, and LUMO+1 for **10f**. Orbital energies [eV] are indicated.

lustrates selected molecular orbitals: HOMO, HOMO−1, LUMO, and LUMO+1 for **10f**. The HOMO (α−187) is largely distributed over the cobalt d_{z^2} orbitals and the π system of the alkyne and pyrimidine base. The LUMO (α−188) is primarily distributed over the cobalt $d_{xz/yz}$ orbitals and the π system of the alkyne group and represents an antibonding orbital between the cobalt centers. HOMO−1 (α−186) represents the bonding interaction between the cobalt $d_{xz/yz}$ orbitals. The HOMO–LUMO gap for **10f** is large (4.25 eV) consistent with high kinetic stability.[48,49]

2.2. Synthesis of $Co_2(CO)_4$(dppm) Complex

We were intrigued to investigate the effect of coordinating a phosphine ligand to the cobalt complex. Phosphine ligands have been employed in complexes screened for anticancer properties.[50] The affinity of the 1,1-bis(diphenylphosphino)methane (dppm) ligand towards cobalt carbonyls is well known,[51] and to our knowledge, no biological studies have been reported so far for (alkyne)$Co_2(CO)_4$(dppm)-connected compounds. Dicobalt hexacarbonyl alkyne complexes are known to react with dppm; however, we elected first to coordinate dppm to the cobalt carbonyl ligand and, subsequently, to react the product with a free alkyne nucleoside. Accordingly, acyl-containing nucleoside **9h** was combined with $Co_2(CO)_6$(dppm), which was prepared from dicobalt octacarbonyl and dppm in toluene following a known procedure.[52] Workup gave nucleoside **11** in 25% yield (Scheme 2). Although

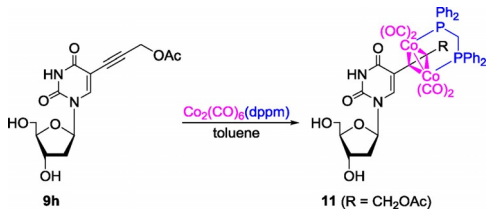

Scheme 2. Synthesis of dppm–dicobalt tetracarbonyl nucleoside **11** from alkyne **9h**.

the presence of dppm in the molecule could enhance the crystallinity, efforts to obtain an X-ray-quality crystal of **11** have not been successful thus far.

The structure of new nucleoside **11** was confirmed by ^{1}H NMR, ^{13}C NMR, ^{31}P NMR, and IR spectroscopy and HRMS. The ^{31}P NMR spectrum features a characteristic resonance at $\delta = 41.05$ ppm in [D_6]DMSO ($\delta = 40.84$ ppm in $CDCl_3$), and this clearly differs from the spectrum of $Co_2(CO)_6$(dppm).[52] The IR spectrum exhibits the characteristic ν_{CO} pattern at $\tilde{\nu} = 2022$, 1990, and 1961 cm^{-1}.[53] Similar to the high-resolution mass spectrum of **10h**, an *m/z* signal for $[M-OAc]^+$ is observed.

2.3. Inhibition of Cell Proliferation

The cytotoxic properties of compounds **9a–h**, **10a–h**, and **11** were tested for their activity in HeLa (human cervix carcinoma), K562 (chronic myelogenous leukemia), and HUVEC (human umbilical vein endothelial cells) cells. As the control (100% viability in the MTT [3-(4,5-dimethylthiazol-2-yl)-2,5-diphenyltetrazolium bromide] assay), cells treated with DMSO (1%) were used. The viability of cells was determined at six different drug concentrations: 2×10^{-1}, 1×10^{-1}, 5×10^{-2}, 1×10^{-2}, 1×10^{-3}, and 1×10^{-4} mM. As the control of the whole experiment, staurosporine (1 μM) was used.

All cobalt compounds displayed significant antiproliferative effects with median inhibitory concentration (IC_{50}) values reaching 20(±5.1) μM (for **10e** in HeLa cells) and 16(±3.5) μM (for **11** in K562 cells). Thus, the potency of the more active target compounds is well within the range of established anticancer drugs such as cisplatin, 20(±6.0) and 40(±7.0) μM in HeLa and K562 cells, respectively (Table 2).

The structure–reactivity relationship seems not to be straightforward. The lead compound for cytotoxic hexacarbonyl dicobalt complexes was diphenyl-substituted **10e** (IC_{50} values in the range of 18 to 20 μM in this assay). HeLa cells were less sensitive towards the structure of metallonucleosides than K562 cells (20–80 vs. 18–30 μM, respectively). Cobalt nucleosides **10c**, **10d**, and **10f** showed selectivity towards K562 cells and were less active in HeLa cells. This selectivity almost disappeared for derivative **10e**, as good antiproliferative effects could be noted in both cells.

For corresponding cobalt carbonyl species **10h** and its dppm homologue **11**, the antiproliferative activity was slightly increased for the latter (IC_{50} values from 30 to 25 μM and from 22 to 16 μM); however, toxicity against HUVEC cells also increased. Interestingly, dppm derivative **11**, containing fewer carbonyl groups than **10h**, was more active in both tumor cell cultures investigated (Table 2).

In regard to the alkyne precursors, preliminary results obtained for noncoordinated alkynyluridines **9a–h** were all above >100 μM; thus, no further screening was attempted. Clearly, coordination of the alkynes to $Co_2(CO)_6$ has a strong influence on the biological activity of the respective alkyne compounds. In general, the coordination process led to a significant increase in the cytotoxic potency for all substituents at the nonnucleoside side of the alkyne.

Table 2. Cytotoxic activity (effect of the substituents) of cobalt nucleosides **10a–h** and **11** for the proliferation of the HeLa, K562, and HUVEC cell lines after incubating for 48 h.

Compound	IC_{50}[a] [μM]		
	HeLa	K562	HUVEC
10a	34 ± 3.4	28 ± 4.3	40 ± 7.6
10a + NAC (1 mM)	140 ± 8.4	90 ± 7.5	
10a + NAC (2 mM)	> 200	> 200	
10b	28 ± 4.5	18 ± 3.6	20 ± 2.0
10c	80 ± 6.1	29 ± 4.7	40 ± 4.8
10d	80 ± 6.5	25 ± 3.6	31 ± 3.1
10e	20 ± 5.1	18 ± 1.9	16 ± 2.6
10f	80 ± 5.7	30 ± 3.7	35 ± 5.1
10g	50 ± 4.6	28 ± 4.8	20 ± 3.8
10h	30 ± 5.0	22 ± 4.7	37 ± 5.5
11	25 ± 3.2	16 ± 3.5	7 ± 5.2
cisplatin	20 ± 6.0	40 ± 7.0	30 ± 6.5

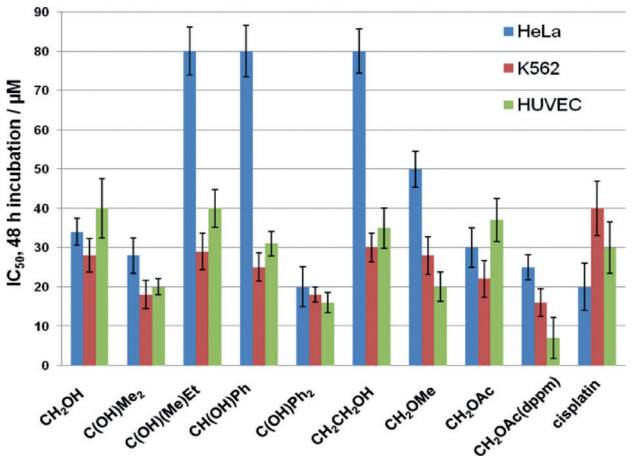

[a] Results were obtained in two separate experiments, each $n = 6$.

2.4. Oxidative Stress

Uncontrolled production of reactive oxygen species (ROS) in cells results in oxidative stress that impairs cellular functions and contributes to the development of cancer, chronic disease, and toxicity.[54,55] Growing evidence suggests that cancer cells exhibit increased intrinsic ROS stress, due in part to oncogenic stimulation, increased metabolic activity, and mitochondrial malfunction.[54] Given that the mitochondrial respiratory chain (electron-transport complexes) is a major source of ROS generation in cells, the vulnerability of mitochondrial DNA to ROS-mediated damage appears to be a mechanism to amplify ROS stress in cancer cells. As this state of oxidative stress makes cancer cells vulnerable to agents that further augment ROS levels, the use of pro-oxidant agents is emerging as an exciting strategy to target tumor cells selectively.[55,56] Accumulation of peroxides and free radicals leads to death of cancer cells, for example, by apoptosis. This biochemical aspect can be exploited to develop novel therapeutic drugs to target cancer cells preferentially and selectively through ROS-mediated mechanisms.[56,57] The contribution of reactive oxygen species to the antitumor activity of many chemotherapeutic agents commonly used in treatment has already been documented.[56]

To gain insight into the induction of oxidative stress, which may be responsible for part of the antiproliferative activity of the investigated compounds against human cancer cells, the levels of reactive oxygen species in the presence of cytotoxic compounds **10a–h** and **11**, as well as representative free-alkyne corresponding nucleoside **9c**, were determined in K562 (chronic myelogenous leukemia) cells by using DCFDA (2,7-dichlorofluorescein diacetate) dye assay. After staining, the cells were incubated for 4 h with the test compounds at concentrations of 5, 10, 20, 50, 100, and 200 μM. Cells treated with 50 and 100 μM H_2O_2 served as positive controls. All cobalt compounds showed a significant increase in the level of reactive oxygen species, which is confirmed by the DCF (2,7-dichlorofluorescein) fluorescence intensity values shown in Table 3.

The DCF fluorescence intensity in the presence of the tested cobalt compounds (1.1 ± 0.07 to 5.2 ± 0.06-fold change in relation to control cells) was comparable to the value for the positive control (i.e. H_2O_2, 3.7 ± 0.10- to 6.1 ± 0.17-fold change in relation to control cells), which is one of the reactive forms of oxygen. The DCF fluorescence intensity increased for all of the tested cobalt compounds upon increasing the concentration of the cobalt complexes. Studies showed that compound **11** (1.4 ± 0.10- to 5.2 ± 0.06-fold change in relation to control cells) was the most potent inducer of oxidative stress in K562 cells.

Confirmation that one of the major mechanisms of action of cobalt nucleoside derivatives involved overproduction of ROS was sought. Therefore, the effect of representative compound **10a** in the presence of a generalized intracellular ROS inhibitor was investigated. HeLa and K562 cancer cells were incubated in the presence of *N*-acetyl-L-cysteine (NAC). Pretreatment of HeLa and K562 cells (30 min) with NAC solutions (1 or 2 mM) enhanced their viability by 20–51 and 10–56%, respectively, compared to treatment with **10a** alone (Figure 4). Thus, the role of ROS induction in the potency of the cobalt complexes was confirmed.

Also, non-cobalt nucleoside derivative **9c** was studied, and this compound did not increase the level of reactive oxygen species (0.9 ± 0.03-fold change in relation to control cells). This result confirms that the cobalt atom present in the structure is responsible for the pro-oxidative properties of the cobalt nucleosides. In conclusion, the results show that the mechanism of action of most antiproliferative cobalt compounds in leukemia cells (K562) may be related to the induction of oxidative stress.

3. Conclusions

Novel 5-oxopropynyl-substituted 2′-deoxyuridines containing alkyl and aryl substituents at the propargyl carbon atom and hydroxy, methoxy, and acetoxy groups were synthesized and converted into their dicobalt hexacarbonyl derivatives. X-ray crystallography confirmed the structure of the cobalt nucleoside containing the homopropargyl alcohol (but-3-yn-1-ol) unit (see compound **10f**) and determined the conformation and hydrogen bonding present in the solid state. The acetoxy cobalt derivative was converted into the corresponding complex containing a bidentate 1,1-bis-(diphenylphosphino)-

Table 3. Oxidative stress of cobalt nucleosides **10a–h** and **9c** (bar plot for 100 μM).

Compound	DCF fluorescence intensity[a]					
	5 μM	10 μM	20 μM	50 μM	100 μM	200 μM
DMSO + DCFDA	1 ± 0.0[b]					
H_2O_2				3.7 ± 0.10[c]	6.1 ± 0.17[d]	
9c	0.9 ± 0.01	0.9 ± 0.03	0.9 ± 0.02	0.9 ± 0.02	0.9 ± 0.03	0.9 ± 0.04
10a	1.2 ± 0.06	1.7 ± 0.19	1.9 ± 0.03	3.2 ± 0.02	3.6 ± 0.09	3.8 ± 0.04
10b	1.2 ± 0.03	1.6 ± 0.42	1.7 ± 0.04	3.0 ± 0.04	3.6 ± 0.06	4.2 ± 0.09
10c	1.2 ± 0.05	1.7 ± 0.19	2.1 ± 0.14	3.5 ± 0.04	4.3 ± 0.02	4.7 ± 0.01
10d	1.3 ± 0.15	1.6 ± 0.13	2.1 ± 0.17	3.5 ± 0.05	4.2 ± 0.07	4.7 ± 0.09
10e	1.2 ± 0.03	1.5 ± 0.01	1.9 ± 0.04	3.5 ± 0.09	4.0 ± 0.04	4.9 ± 0.03
10f	1.3 ± 0.18	1.6 ± 0.17	2.0 ± 0.12	3.2 ± 0.02	3.8 ± 0.04	4.1 ± 0.02
10g	1.2 ± 0.03	1.6 ± 0.18	1.7 ± 0.04	3.2 ± 0.05	3.6 ± 0.04	4.1 ± 0.04
10h	1.1 ± 0.07	1.3 ± 0.03	1.7 ± 0.04	3.0 ± 0.04	3.4 ± 0.01	3.9 ± 0.03
11	1.4 ± 0.10	1.6 ± 0.01	2.5 ± 0.02	3.7 ± 0.06	4.2 ± 0.02	5.2 ± 0.06

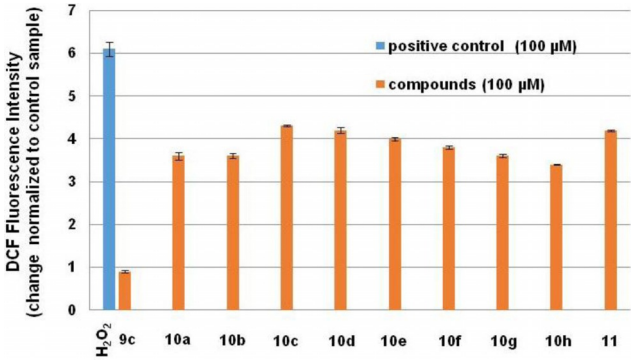

[a] Change normalized to control sample. [b] Control, concentration 1% DMSO, 20 μM DCFDA. [c] Positive control, concentration 50 μM. [d] Positive control, concentration 100 μM.

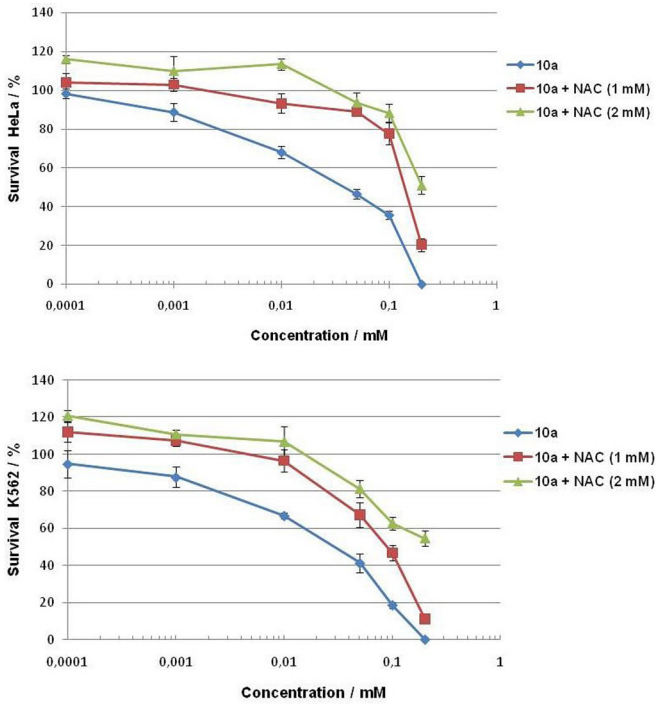

Figure 4. Survival rate of HeLa (top) and K562 (bottom) cells after incubating with compounds **10a** and **10a** + NAC (1 or 2 mM) for 48 h.

methane (dppm) ligand. It was demonstrated that the presence of the cobalt carbonyl was essential to achieve a cytotoxic effect, as the alkynyl precursor did not exhibit pronounced activity against HeLa and K562 human cancer cells in vitro, with higher efficacy seen in the last one. Similar to the results obtained for other cobalt carbonyl complexes, the activity depended on the presence of the cobalt carbonyl moiety, suggesting that metal carbonyls are useful functional groups for modifying or inducing biological activity.

Experimental Section

General Instrumentation

All NMR spectroscopy measurements were performed with a Bruker Avance III 500 spectrometer operating at 500.13 MHz for ^{1}H, 125.75 MHz for ^{13}C, and 202.45 MHz for ^{31}P at 22 °C. Mass spectra were recorded with an Agilent 6520 Q-TOF LC–MS (HRMS). FTIR spectra were recorded with ATI Mattson Infinity Series AR60, Thermo-Scientific Nicolet 6700 ATR, and Bruker Alpha-P ATR spectrometers. All products were stored in a refrigerator (4 °C).

Syntheses

General Procedure for the Synthesis of 2′-Deoxy-5-alkynyluridines 9a–h

A round-bottomed flask was charged with 2′-deoxy-5-iodouridine (**I-dU**; 2.09 g, 5.90 mmol), $Pd(PPh_3)_4$ (0.690 g, 0.597 mmol), CuI (0.120 g, 0.628 mmol), DMF (15 mL), Et_3N (1.8 mL, 12 mmol), and the respective terminal alkyne. The mixture was stirred at 40 °C for 22 h (oil bath). The solvent was removed (by oil pump vacuum), and the residue was dissolved in chloroform (10 mL) and kept in the freezer (−4 °C) for 12 h. The precipitate was filtered off and washed with cold chloroform (3 × 3 mL). The mother liquor was concentrated and subjected to column chromatography (230–400 mesh silica gel, 0→12% MeOH/$CHCl_3$). The product was dried by oil pump vacuum for 2 h to give **9a–h**.

2′-Deoxy-5-(3-hydroxyprop-1-yn-1-yl)uridine (**9a**): From 2-propyn-1-ol (propargyl alcohol, 0.86 mL, 14.8 mmol). Yield: 0.830 g, 2.94 mmol (50%). R_f = 0.25 ($CHCl_3$/MeOH 7:1). ^{1}H NMR ([D_6]DMSO): δ = 11.57 (s, 1H, N-H), 8.14 (s, 1H, H-6), 6.07 (t, J = 6.5 Hz, 1H, H-1′), 5.26 (t, J = 6.1 Hz, 1H, OH-3′), 5.21 (d, J = 4.51 Hz, 1H, OH), 5.08 (t, J = 5.15 Hz, 1H, OH-5′), 4.20 (s, 2H, CH_2), 4.19 (s, 1H, H-3′), 3.77–3.74 (m, 1H, H-4′), 3.60–3.55 (m, 1H, H-5′), 3.54–3.49 (m, 1H, H-5″), 2.10–2.06 ppm (m, 2H, H-2′, H-2″); ^{13}C NMR ([D_6]DMSO): δ = 163.10, 150.91, 144.99, 99.69, 93.97, 89.06, 86.15, 77.80, 71.67, 62.44, 50.96, 40.38 ppm; IR (KBr): $\tilde{\nu}$ = 3401 (br m), 2924 (m), 1726 (s), 1667 (s), 1468 (m), 1279 (m), 1051 (m) cm^{-1}; HRMS (ESI-TOF): m/z: calcd for $C_{12}H_{15}N_2O_6$: 283.0925 $[M+H]^+$; found: 283.0927; elemental analysis calcd (%) for $C_{12}H_{14}N_2O_6$ (282.25): C 51.07, H 5.00, N 9.93; found: C 51.18, H 5.49, N 9.79.

2′-Deoxy-5-(3-hydroxy-3-methylbut-1-yn-1-yl)uridine (**9b**): From 2-methyl-3-butyn-2-ol (1.43 mL, 14.8 mmol). Yield: 0.750 g, 2.42 mmol (41%). R_f = 0.27 ($CHCl_3$/MeOH 8:1). ^{1}H NMR ([D_6]DMSO): δ = 11.54 (s, 1H, N-H), 8.10 (s, 1H, H-6), 6.07 (t, J = 6.9 Hz, 1H, H-1′),

5.36 (s, 1H, OH), 5.23–5.20 (m, 1H, OH-3′), 5.09–5.05 (m, 1H, OH-5′), 4.21–4.17 (m, 1H, H-3′), 3.77–3.74 (m, 1H, H-4′), 3.60–3.55 (m, 1H, H-5′), 3.54–3.50 (m, 1H, H-5″), 2.09–2.05 (m, 2H, H-2′, H-2″), 1.37 ppm (s, 6H, CH_3); ^{13}C NMR ([D$_6$]DMSO): δ = 161.59, 149.54, 143.28, 98.61, 98.49, 87.60, 84.70, 79.23, 73.15, 70.19, 63.71, 60.99, 31.68 ppm; IR (KBr): $\tilde{\nu}$ = 3418 (brm), 2982 (m), 1706 (s), 1467 (m), 1283 (m), 1093 cm^{-1} (m); HRMS (ESI-TOF): *m/z*: calcd for $C_{14}H_{19}N_2O_6$: 311.1238 [*M*+H]$^+$; found: 311.1236.

2′-Deoxy-5-(3-hydroxy-3-methylpent-1-yn-1-yl)uridine (**9c**): From 3-methyl-1-pentyn-3-ol (1.68 mL, 14.8 mmol). Yield: 1.07 g, 3.30 mmol (56%). R_f = 0.39 ($CHCl_3$/MeOH 8:1). ^{1}H NMR ([D$_6$]DMSO): δ = 11.56 (s, 1H, N-H), 8.13 (s, 1H, H-6), 6.10 (t, *J* = 6.6 Hz, 1H, H-1′), 5.27–5.22 (m, 2H, CH_2), 5.09 (brs, 1H, OH-3′), 4.22 (brs, 1H, OH-5′), 3.78 (brs, 1H, H-3′), 3.62–3.58 (m, 1H, H-5′), 3.57–3.53 (m, 1H, H-5″), 2.11 (dd, *J* = 5.8, 5.4 Hz, 1H, H-4′), 1.62–1.51 (m, 2H, H-2′, H-2″), 1.34 (s, 3H, CH_3), 0.95 ppm (dd, *J* = 7.4 Hz, 3H, CH_3); ^{13}C NMR ([D$_6$]DMSO): δ = 161.57, 149.51, 143.17, 98.53, 97.47, 87.59, 84.69, 79.23, 74.29, 70.13, 67.22, 60.94, 36.47, 29.31, 9.10 ppm; IR (KBr): $\tilde{\nu}$ = 3348 (brm), 2973 (m), 1668 (s), 1461 (s), 1275 (m), 1089 cm^{-1} (m); HRMS (ESI-TOF): *m/z*: calcd for $C_{15}H_{21}N_2O_6$: 325.1395 [*M*+H]$^+$; found: 325.1397.

2′-Deoxy-5-(3-hydroxy-3-phenylprop-1-yn-1-yl)uridine (**9d**): From 1-phenyl-2-propyn-1-ol (1.80 mL, 14.8 mmol). Yield: 0.972 g, 2.72 mmol (46%). R_f = 0.59 ($CHCl_3$/MeOH 8:1). ^{1}H NMR ([D$_6$]DMSO): δ = 11.61 (s, 1H, N-H), 8.20 and 8.19 (2s, 1H, H-6), 7.53–7.40 (m, 2H, Ph), 7.36–7.28 (m, 2H, Ph), 7.27–7.21 (m, 1H, Ph), 6.12–6.06 (m, 2H, H-1′, OH), 5.51 (d, *J* = 6.22 Hz, 1H, OH-3′), 5.23 (d, *J* = 4.48 Hz, 1H, OH-5′), 5.10 (t, *J* = 4.98 Hz, 1H, CH), 4.23–4.19 (m, 1H, H-3′), 3.79–3.76 (m, 1H, H-4′), 3.62–3.57 (m, 1H, H-5′), 3.57–3.52 (m, 1H, H-5″), 2.13–2.07 ppm (m, 2H, H-2′, H-2″); ^{13}C NMR ([D$_6$]DMSO): δ = 161.69, 149.56, 143.69, 141.97, 128.48, 128.31, 127.69, 126.76, 126.19, 98.23, 93.96, 87.73, 84.88, 79.26, 77.47, 70.25, 63.13, 61.06 ppm; IR (KBr): $\tilde{\nu}$ = 3345 (brm), 3061 (m), 2824 (m), 1668 (s), 1454 (s), 1278 (m), 1088 cm^{-1} (m); HRMS (ESI-TOF): *m/z*: calcd for $C_{18}H_{17}N_2O_5$: 341.1132 [*M*−OH]$^+$; found: 341.1133.

2′-Deoxy-5-(3-hydroxy-3,3-diphenylprop-1-yn-1-yl)uridine (**9e**): From 1,1-diphenyl-2-propyn-1-ol (3.10 g, 14.8 mmol). Yield: 2.36 g, 5.43 mmol (92%). R_f = 0.23 ($CHCl_3$/MeOH 9:1). ^{1}H NMR ([D$_6$]DMSO): δ = 11.68 (s, 1H, N-H), 8.29 (s, 1H, H-6), 7.63–7.59 (m, 4H, Ph), 7.33–7.28 (m, 4H, Ph), 7.23–7.19 (m, 2H, Ph), 6.85 (s, 1H, OH), 6.14 (t, *J* = 6.7 Hz, 1H, H-1′), 5.26 (brs, 1H, OH-3′), 5.12 (brs, 1H, OH-5′), 4.26 (brs, 1H, H-3′), 3.83–3.80 (m, 1H, H-4′), 3.65–3.61 (m, 1H, H-5′), 3.60–3.56 (m, 1H, H-5″), 2.18–2.13 ppm (m, 2H, H-2′, H-2″); ^{13}C NMR ([D$_6$]DMSO): δ = 161.72, 149.51, 146.36, 143.47, 128.01, 127.07, 125.77, 98.12, 96.11, 87.72, 84.92, 79.26, 78.40, 73.28, 70.15, 60.97, 45.79, 8.74 ppm; IR (KBr): $\tilde{\nu}$ = 3342 (brm), 3056 (m), 2931 (m), 1668 (s), 1449 (s), 1276 (m), 1029 cm^{-1} (m); HRMS (ESI-TOF): *m/z*: calcd for $C_{24}H_{21}N_2O_5$: 417.1445 [*M*−OH]$^+$; found: 417.1447.

2′-Deoxy-5-(4-hydroxybut-1-yn-1-yl)uridine (**9f**): From 3-butyn-1-ol (1.12 mL, 14.8 mmol). Yield: 0.943 g, 3.18 mmol (54%). R_f = 0.31 ($CHCl_3$/MeOH 8:1). ^{1}H NMR ([D$_6$]DMSO): δ = 11.50 (s, 1H, N-H), 8.07 (s, 1H, H-6), 6.07 (t, *J* = 6.7 Hz, 1H, H-1′), 5.20 (brs, 1H, OH-3′), 5.04 (brs, 1H, OH-5′), 4.81 (brs, 1H, OH), 4.19 (brs, 1H, H-3′), 3.77–3.72 (m, 1H, H-4′), 3.59–3.46 (m, 4H, H-5′, H-5″, CH_2), 2.48–2.42 (m, 2H, CH_2), 2.10–2.03 ppm (m, 2H, H-2′, H-2″); ^{13}C NMR ([D$_6$]DMSO): δ = 161.89, 149.55, 143.00, 99.03, 91.08, 87.61, 84.65, 73.51, 70.29, 61.08, 59.80, 56.14, 45.84, 23.49 ppm; IR (KBr): $\tilde{\nu}$ = 3333 (brm), 3060 (m), 2931 (m), 1668 (s), 1463 (s), 1277 (m), 1037 cm^{-1} (m); HRMS (ESI-TOF): *m/z*: calcd for $C_{13}H_{17}N_2O_6$: 297.1082 [*M*+H]$^+$; found: 297.1080.

2′-Deoxy-5-(3-methoxyprop-1-yn-1-yl)uridine (**9g**):[47] From methyl propargyl ether (1.25 mL, 14.8 mmol). Yield: 1.20 g, 4.05 mmol (69%). R_f = 0.43 ($CHCl_3$/MeOH 7:1). ^{1}H NMR ([D$_6$]DMSO): δ = 11.59 (s, 1H, N-H), 8.22 (s, 1H, H-6), 6.07 (t, *J* = 6.4 Hz, 1H, H-1′), 5.21 (brs, 1H, OH-3′), 5.08 (brs, 1H, OH-5′), 4.21 (s, 2H, CH_2), 4.19 (brs, 1H, H-3′), 3.76 (dd, *J* = 3.6 Hz, 1H, H-4′), 3.61–3.56 (m, 1H, H-5′), 3.55–3.50 (m, 1H, H-5″), 3.24 (s, 3H, OCH_3), 2.11–2.07 ppm (m, 2H, H-2′, H-2″); ^{13}C NMR ([D$_6$]DMSO): δ = 161.67, 149.51, 144.13, 97.82, 88.65, 87.66, 84.85, 78.77, 70.09, 60.93, 59.63, 56.97, 40.23 ppm; IR (KBr): $\tilde{\nu}$ = 3394 (brm), 2993 (m), 1703 (s), 1680 (s), 1468 (m), 1294 (m), 1080 cm^{-1} (m); HRMS (ESI-TOF): *m/z*: calcd for $C_{13}H_{17}N_2O_6$: 297.1082 [*M*+H]$^+$; found: 297.1080; elemental analysis calcd (%) for $C_{13}H_{16}N_2O_6$ (296.275): C 52.70, H 5.44, N 9.46; found: C 52.49, H 5.87, N 9.51.

2′-Deoxy-5-[3-(acetyloxy)prop-1-yn-1-yl]uridine (**9h**): From propargyl acetate (1.47 mL, 14.8 mmol). Yield: 1.26 g, 3.89 mmol (66%). R_f = 0.54 ($CHCl_3$/MeOH 7:1). ^{1}H NMR ([D$_6$]DMSO): δ = 11.62 (s, 1H, N-H), 8.22 (s, 1H, H-6), 6.06 (t, *J* = 6.5 Hz, 1H, H-1′), 5.21 (brs, 1H, OH-3′), 5.08 (brs, 1H, OH-5′), 4.83 (s, 2H, CH_2), 4.21–4.16 (m, 1H, H-3′), 3.77–3.74 (m, 1H, H-4′), 3.61–3.55 (m, 1H, H-5′), 3.54–3.50 (m, 1H, H-5″), 2.11–2.06 (m, 2H, H-2′, H-2″), 2.02 ppm (s, 3H, CH_3); ^{13}C NMR ([D$_6$]DMSO): δ = 169.83, 161.50, 149.48, 144.73, 97.36, 87.70, 86.84, 84.92, 78.93, 70.13, 60.96, 52.37, 20.54 ppm; IR (KBr): $\tilde{\nu}$ = 3442 (m), 3389 (m), 2987 (m), 2823 (m), 1701 (s), 1627 (s), 1467 (m), 1288 (m), 1052 cm^{-1} (m); HRMS (ESI-TOF): *m/z*: calcd for $C_{14}H_{17}N_2O_7$: 325.1031 [*M*+H]$^+$; found: 325.1028; elemental analysis calcd (%) for $C_{14}H_{16}N_2O_7$ (324.29): C 51.85, H 4.97, N 8.64; found: C 51.58, H 5.19, N 8.73.

General Procedure for the Synthesis of Dicobalt Hexacarbonyl 2′-Deoxy-5-alkynyluridines 10a–h

Under a nitrogen atmosphere, a round-bottomed flask was charged with $Co_2(CO)_8$ (0.690 g, 2.02 mmol), **9a–h** (1.69 mmol), and THF (18 mL). The mixture was stirred at room temperature (22 °C) for 1 h. The solvent was removed by rotary evaporation. Column chromatography (230–400 mesh silica gel, 0→5% MeOH/$CHCl_3$) gave **10a–h** as a red-brown compound.

Dicobalt hexacarbonyl 2′-deoxy-5-(3-hydroxyprop-1-yn-1-yl)uridine (**10a**): From compound **9a** (0.477 g, 1.69 mmol). Yield: 0.557 g, 0.98 mmol (58%). R_f = 0.75 ($CHCl_3$/MeOH 7:1). ^{1}H NMR ([D$_6$]DMSO): δ = 11.60 (s, 1H, NH), 8.18 (s, 1H, H-6), 6.17 (brs, 1H, H-1′), 5.53 (brs, 1H, OH-3′), 5.24 (brs, 1H, OH-5′), 5.04 (brs 1H, OH), 4.73 (brs, 2H, CH_2), 4.23 (brs, 1H, H-3′), 3.84 (brs, 1H, H-4′), 3.59–3.44 (m, 2H, H-5′, H-5″), 2.16 (brs, 1H, H-2′), 2.02 ppm (brs, 1H, H-2″); ^{13}C NMR ([D$_6$]DMSO): δ = 200.25, 161.27, 150.21, 139.69, 111.64, 103.36, 88.49, 85.52, 82.63, 79.63, 71.49, 62.52, 62.08, 40.83, 40.20 ppm; IR (KBr): $\tilde{\nu}$ = 3421 (brm), 2927 (w), 2094 (s), 2054 (s), 2026 (s), 1693 (m), 1456 (m), 1276 (m), 1095 cm^{-1} (m); HRMS (ESI-TOF): *m/z*: calcd for $C_{18}H_{13}Co_2N_2O_{11}$: 550.9178 [*M*−OH]$^+$; found: 550.9173; elemental analysis calcd (%) for $C_{18}H_{14}Co_2N_2O_{12}$ (568.18): C 38.05, H 2.48, N 4.93; found: C 37.27, H 2.52, N 5.13.

Dicobalt hexacarbonyl 2′-deoxy-5-(3-hydroxy-3-methylbut-1-yn-1-yl)uridine (**10b**): From compound **9b** (0.524 g, 1.69 mmol). Yield: 0.312 g, 0.52 mmol (31%). R_f = 0.53 ($CHCl_3$/MeOH 8:1). ^{1}H NMR ([D$_6$]DMSO): δ = 11.79 (s, 1H, NH), 8.27 (s, 1H, H-6), 6.20–6.15 (m, 1H, H-1′), 5.74 (brs, 1H, OH), 5.25 (brs, 1H, OH-3′), 5.02 (brs, 1H, OH-5′), 4.23 (brs, 1H, H-3′), 3.84 (brs, 1H, H-4′), 3.58–3.45 (m, 2H, H-5′, H-5″), 2.21–2.14 (m, 1H, H-2′), 2.02–1.94 (m, 1H, H-2″), 1.46 ppm (s, 6H, CH_3); ^{13}C NMR ([D$_6$]DMSO): δ = 199.88, 161.55, 149.68, 140.12, 111.23, 110.50, 88.08, 85.02, 83.38, 79.24, 71.78,

71.23, 61.83, 31.84, 31.64 ppm; IR (KBr): $\tilde{\nu}$ = 3383 (br m), 2975 w, 2093 (s), 2056 (s), 2019 (s), 1651 (m), 1461 (m), 1287 (m), 1101 cm^{-1} (m); HRMS (ESI-TOF): *m/z*: calcd for $C_{20}H_{17}Co_2N_2O_{11}$: 578.9491 $[M-OH]^+$; found: 578.9494; elemental analysis calcd (%) for $C_{20}H_{18}Co_2N_2O_{12}$ (596.23): C 40.29, H 3.04, N 4.70; found: C 39.90, H 3.29, N 4.29.

Dicobalt hexacarbonyl 2′-deoxy-5-(3-hydroxy-3-methylpent-1-yn-1-yl)uridine (**10c**): From compound **9c** (0.548 g, 1.69 mmol). Yield: 0.660 g, 1.08 mmol (64%). R_f = 0.78 ($CHCl_3$/MeOH 8:1). ^{1}H NMR ([D$_6$]DMSO): δ = 11.86 (s, 1H, N-H), 8.30 and 8.27 (2s, 1H, H-6), 6.26–6.17 (m, 1H, H-1′), 5.69 (d, *J* = 5.7 Hz, 1H, OH), 5.27 (br s, 1H, OH-3′), 5.06 (br s, 1H, OH-5′), 4.26 (br s, 1H, H-3′), 3.90–3.84 (m, 1H, H-4′), 3.61–3.55 (m, 1H, H-5′), 3.54–3.46 (m, 1H, H-5″), 2.23–2.17 (m, 1H, CH_2), 2.05–1.96 (m, 1H, CH_2), 1.74–1.61 (m, 2H, H-2′, H-2″), 1.42 (s, 3H, CH_3), 0.90 ppm (d, *J* = 7.0 Hz, 3H, CH_3); ^{13}C NMR ([D$_6$]DMSO): δ = 199.57, 161.42, 149.33, 139.95, 111.23, 110.61, 87.82, 84.94, 83.60, 79.01, 73.44, 71.03, 61.55, 36.28, 28.98, 8.11 ppm; IR (KBr): $\tilde{\nu}$ = 3353 (br m), 2979 (m), 2091 (m), 2050 (s), 2004 (vs), 1665 (s), 1459 (s), 1273 (m), 1098 cm^{-1} (m); HRMS (ESI-TOF): *m/z*: calcd for $C_{21}H_{19}Co_2N_2O_{11}$: 592.9648 $[M-OH]^+$; found: 592.9650.

Dicobalt hexacarbonyl 2′-deoxy-5-(3-hydroxy-3-phenylprop-1-yn-1-yl)uridine (**10d**): From compound **9d** (0.605 g, 1.69 mmol). Yield: 0.773 g, 1.20 mmol (71%). R_f = 0.71 ($CHCl_3$/MeOH 8:1). ^{1}H NMR ([D$_6$]DMSO): δ = 11.75 (s, 1H, N-H), 8.17 and 8.11 (2s, 1H, H-6), 7.34–7.21 (m, 4H, Ph), 7.18–7.11 (m, 1H, Ph), 6.24–6.15 (m, 2H, H-1′, OH), 6.12 (br s, 1H, OH-3′), 5.23 (br s, 1H, OH-5′), 4.97 (br s, 1H, CH), 4.27–4.17 (m, 1H, H-3′), 3.87–3.77 (m, 1H, H-4′), 3.55–3.44 (m, 1H, H-5′), 3.42–3.34 (m, 1H, H-5″), 2.19–2.12 (m, 1H, H-2′), 2.04–1.88 ppm (m, 1H, H-2″); ^{13}C NMR ([D$_6$]DMSO): δ = 199.45, 198.93, 160.78, 149.48, 145.60, 139.22, 127.79, 127.74, 126.87, 125.16, 111.91, 111.64, 108.26, 87.70, 84.41, 83.06, 78.94, 71.88, 71.75, 61.54 ppm; IR (KBr): $\tilde{\nu}$ = 3364 (br m), 3030 (br m), 2092 (m), 2052 (s), 2004 (vs), 1659 (s), 1453 (s), 1272 (m), 1034 cm^{-1} (m); HRMS (ESI-TOF): *m/z*: calcd for $C_{24}H_{17}Co_2N_2O_{11}$: 626.9491 $[M-OH]^+$; found: 626.9489; elemental analysis calcd (%) for $C_{24}H_{18}Co_2N_2O_{12}$ (644.27): C 44.74, H 2.82, N 4.35; found: C 44.35, H 2.73, N 4.44.

Dicobalt hexacarbonyl 2′-deoxy-5-(3-hydroxy-3,3-diphenylprop-1-yn-1-yl)uridine (**10e**): From compound **9e** (0.734 g, 1.69 mmol). Yield: 0.754 g, 1.05 mmol (62%). R_f = 0.53 ($CHCl_3$/MeOH 9:1). ^{1}H NMR ([D$_6$]DMSO): δ = 12.02 (s, 1H, N-H), 8.35 (s, 1H, H-6), 7.41–7.23 (m, 10H, 2Ph), 7.21 (s, 1H, OH), 6.24 (t, *J* = 6.7 Hz, 1H, H-1′), 5.29 (br s, 1H, OH-3′), 5.07 (br s, 1H, OH-5′), 4.27 (br s, 1H, H-3′), 3.89 (br s, 1H, H-4′), 3.57–3.51 (m, 1H, H-5′), 3.49–3.43 (m, 1H, H-5″), 2.29–2.22 (m, 1H, H-2′), 2.09–2.02 ppm (m, 1H, H-2″); ^{13}C NMR ([D$_6$]DMSO): δ = 198.82, 161.80, 149.27, 146.63, 140.13, 127.75, 127.16, 127.05, 126.87, 111.61, 110.06, 87.92, 85.77, 85.04, 79.50, 78.96, 70.95, 61.38 ppm; IR (KBr): $\tilde{\nu}$ = 3341 (br m), 3054 (m), 2092 (m), 2052 (s), 2007 (vs), 1661 (s), 1447 (s), 1273 (m), 1091 cm^{-1} (m); HRMS (ESI-TOF): *m/z*: calcd for $C_{30}H_{21}Co_2N_2O_{11}$: 702.9804 $[M-OH]^+$; found: 702.9800.

Dicobalt hexacarbonyl 2′-deoxy-5-(4-hydroxybut-1-yn-1-yl)uridine (**10f**): From compound **9f** (0.500 g, 1.69 mmol). Yield: 0.531 g, 0.91 mmol (54%). R_f = 0.54 ($CHCl_3$/MeOH 8:1). ^{1}H NMR ([D$_6$]DMSO): δ = 11.56 (s, 1H, N-H), 8.19 (s, 1H, H-6), 6.22–6.14 (m, 1H, H-1′), 5.22 (br s, 1H, OH-3′), 5.04 (br s, 1H, OH-5′), 4.77 (br s, 1H, H-3′), 4.24 (br s, 1H, H-4′), 3.83 (br s, 1H, OH), 3.67–3.45 (m, 4H, H-5′, H-5″, CH_2), 3.10 (br s, 2H, CH_2), 2.18–2.09 (m, 1H, H-2′), 2.06–1.97 ppm (m, 1H, H-2″); ^{13}C NMR ([D$_6$]DMSO): δ = 199.35, 160.19, 149.36, 138.34, 111.06, 98.59, 87.57, 84.50, 83.80, 78.73, 70.72, 61.41, 61.23, 36.25 ppm; IR (KBr): $\tilde{\nu}$ = 3358 (br m), 2945 (m), 2089 (m), 2047 (s), 1994 (vs), 1668 (s), 1455 (s), 1273 (m), 1052 cm^{-1} (m); HRMS (ESI-TOF): *m/z*: calcd for $C_{19}H_{17}Co_2N_2O_{12}$: 582.9440 $[M+H]^+$; found: 582.9441; elemental analysis calcd (%) for $C_{19}H_{16}Co_2N_2O_{12}$ (582.20): C 39.20, H 2.77, N 4.81; found: C 38.97, H 3.08, N 4.98.

Dicobalt hexacarbonyl 2′-deoxy-5-(3-methoxyprop-1-yn-1-yl)uridine (**10g**): From compound **9g** (0.500 g, 1.69 mmol). Yield: 0.812 g, 1.39 mmol (83%). R_f = 0.51 ($CHCl_3$/MeOH 7:1). ^{1}H NMR ([D$_6$]DMSO): δ = 11.59 (s, 1H, *N*-3), 8.19 (s, 1H, H-6), 6.17 (br s, 1H, H-1′), 5.24 (br s, 1H, OH-3′), 5.06 (br s, 1H, OH-5′), 4.67 (s, 2H, CH_2), 4.24 (br s, 1H, H-3′), 3.84 (br s, 1H, H-4′), 3.63–3.46 (m, 2H, H-5′, H-5″), 3.39 (s, 3H, OCH_3), 2.15 (br s, 1H, H-2′), 2.03 ppm (br s, 1H, H-2″); ^{13}C NMR ([D$_6$]DMSO): δ = 199.60, 160.73, 149.83, 139.42, 111.04, 97.01, 88.12, 85.13, 82.54, 72.63, 71.09, 61.66, 58.41 40.51 ppm; IR (KBr): $\tilde{\nu}$ = 3425 (br m), 2933 (w), 2094 (s), 2053 (s), 2026 (s), 1690 (m), 1453 (m), 1275 (m), 1093 cm^{-1} (m); HRMS (ESI-TOF): *m/z*: calcd for $C_{19}H_{17}Co_2N_2O_{12}$: 582.9440 $[M+H]^+$; found: 582.9438; elemental analysis calcd (%) for $C_{19}H_{16}Co_2N_2O_{12}$ (582.20): C 39.20, H 2.77, N 4.81; found: C 39.17, H 2.43, N 5.11.

Dicobalt hexacarbonyl 2′-deoxy-5-[3-(acetyloxy)prop-1-yn-1-yl]uridine (**10h**): From compound **9h** (0.548 g, 1.69 mmol). Yield: 0.856 g, 1.40 mmol (83%). R_f = 0.79 ($CHCl_3$/MeOH 7:1). ^{1}H NMR ([D$_6$]DMSO): δ = 11.63 (s, 1H, NH), 8.22 (s, 1H, H-6), 6.17 (t, *J* = 6.7 Hz, 1H, H-1′), 5.47–5.35 (m, 2H, CH_2), 5.24 (br s, 1H, OH-3′), 5.09–5.04 (m, 1H, OH-5′), 4.24 (br s, 1H, H-3′), 3.84 (br s, 1H, H-4′), 3.59–3.53 (m, 1H, H-5′), 3.53–3.48 (m, 1H, H-5″), 2.20–2.14 (m, 1H, H-2′), 2.08–2.04 (m, 1H, H-2″), 2.03 ppm (s, 3H, CH_3); ^{13}C NMR ([D$_6$]DMSO): δ = 199.22, 170.12, 160.77, 149.79, 139.83, 110.92, 94.91, 88.19, 85.30, 82.43, 79.24, 71.09, 64.92, 61.62, 20.33 ppm; IR (KBr): $\tilde{\nu}$ = 3423 (br m), 2936 (w), 2095 (s), 2056 (s), 2026 (s), 1689 (m), 1454 (m), 1273 (m), 1096 cm^{-1} (m); HRMS (ESI-TOF): *m/z*: calcd for $C_{18}H_{13}Co_2N_2O_{11}$: 550.9178 $[M-OAc]^+$; found: 550.9181; elemental analysis calcd (%) for $C_{20}H_{16}Co_2N_2O_{13}$ (610.21): C 39.37, H 2.64, N 4.59; found: C 39.17, H 2.43, N 5.11.

[Bis(diphenylphosphino)methane] dicobalt tetracarbonyl 2′-deoxy-5-[3-(acetyloxy)prop-1-yn-1-yl]uridine (**11**): Under a nitrogen atmosphere, a 50 mL flask was charged with $Co_2(CO)_8$ (0.500 g, 1.46 mmol), toluene (20 mL), and 1,1-bis(diphenylphosphino)methane (dppm; 0.561 g, 1.46 mmol). The mixture was stirred at room temperature for 3 h. The solvent was removed by rotary evaporation. Column chromatography (230–400 mesh silica gel, 0→2% MeOH/$CHCl_3$) gave $Co_2(CO)_6$(dppm)[52] (0.842 g, 1.26 mmol, 86%).

A 50 mL flask was charged with $Co_2(CO)_6$(dppm) (0.402 g, 0.600 mmol), nucleoside **9h** (0.194 g, 0.600 mmol), and THF (12 mL). The solution was stirred at room temperature (22 °C) for 24 h. The solvent was removed by rotary evaporation. Column chromatography (230–400 mesh silica gel, 0→10% MeOH/$CHCl_3$) gave compound **11** (0.141 g, 0.150 mmol, 25%). R_f = 0.83 ($CHCl_3$/MeOH 9:1). ^{1}H NMR ([D$_6$]DMSO): δ = 11.42 (s, 1H, NH), 7.88 (br s, 1H, H-6), 7.52–7.09 (m, 20H, 4Ph), 6.26–6.17 (m, 1H, H-1′), 5.29 (br s, 2H, CH_2), 4.91 (br s, 1H, OH-3′), 4.23 (br s, 1H, OH-5′), 3.98–3.84 (m, 2H, CH_2), 3.81 (br s, 1H, H-3′), 3.49 (br s, 1H, H-4′), 3.43 (br s, 1H, H-5′), 3.33 (br s, 1H, H-5″), 2.23–2.16 (m, 1H, H-2′), 2.04–1.96 (m, 1H, H-2″), 1.67 ppm (s, 3H, CH_3); ^{13}C NMR ([D$_6$]DMSO): δ = 205.96, 203.42, 201.20, 200.76, 169.55, 160.23, 149.70, 137.20, 137.01, 136.85, 135.85, 131.46, 131.04, 129.20, 129.42, 128.07, 127.87, 116.21, 96.99, 87.40, 84.16, 80.00, 70.94, 67.08, 61.74, 32.97, 23.11, 20.07 ppm; ^{31}P NMR ([D$_6$]DMSO): δ = 41.05 ppm; ^{31}P NMR ($CDCl_3$): δ = 40.84 ppm; IR (KBr): $\tilde{\nu}$ = 3394 (br m), 3054 (w), 2022 (s), 1990 (s), 1961 (vs), 1674 (m), 1433 (m), 1218 (m), 1092 cm^{-1} (m); HRMS (ESI-TOF): *m/z*: calcd for $C_{41}H_{35}Co_2N_2O_9P_2$: 879.0477 $[M-OAc]^+$; found: 879.0476.

Cells and Cytotoxicity Assay

HeLa (human cervix carcinoma) and K562 (chronic myelogenous leukemia) cells were cultured in RPMI 1640 medium supplemented with antibiotics and 10% fetal calf serum (HeLa, K562) under a 5% CO_2/95% air atmosphere. A total of 7×10^3 cells were seeded on each well of a 96-well plate (Nunc). After 24 h, cells were exposed to the test compounds for an additional 48 h. Stock solutions of test compounds were freshly prepared in DMSO. The final concentrations of the compounds tested in the cell cultures were: 2×10^{-1}, 1×10^{-1}, 5×10^{-2}, 1×10^{-2}, 1×10^{-3}, and 1×10^{-4} mM. The concentration of DMSO in the cell culture medium was 1%.

Human umbilical vein endothelial cells (HUVEC) were acquired from Life Technologies and were cultured in Medium 200 with low serum growth supplement (Life Technologies) according to the manufacturer's instructions. A total of 10×10^3 cells were seeded on each well of a 96-well plate (Nunc) in the presence of antibiotics (100 U mL^{-1} penicillin and 100 μg mL^{-1} streptomycin).

The cytotoxicity of each compound was determined by the MTT [3-(4,5-dimethylthiazol-2-yl)-2,5-diphenyltetrazolium bromide, Sigma] assay, as previously described.[58] Briefly, after 24 or 48 h of incubation with the drug, the cells were treated with the MTT reagent and incubation was continued for 2 h. MTT–formazan crystals were dissolved in 20% sodium dodecyl sulfate (SDS) and 50% DMF at pH 4.7, and the absorbance was read at $\lambda=570$ and 650 nm with an ELISA-PLATE READER (FLUOstar Omega). As control (100% viability), cells grown in the presence of only vehicle (1% DMSO) were used.

In a separate assay, the HeLa and K562 cells were pretreated with 1 or 2 mM *N*-acetyl-L-cysteine (NAC), a ROS inhibitor, for 30 min before completing the above steps, following the previously described procedure.[59]

The IC_{50} values (the concentration of test compound required to reduce the cell survival fraction to 50% of the control) were calculated from dose–response curves and were used as a measure of cellular sensitivity to a given treatment.

Intracellular ROS Measurement in Living Cells

Intracellular ROS levels were assessed with a 2,7-dichlorofluorescein diacetate (DCFDA) dye assay. DCFDA (Sigma–Aldrich) is a cell-permeant reagent, a fluorogenic dye that measures the activity of hydroxyl, peroxyl, and other ROS within the cell. After diffusion into the cell, DCFDA was deacetylated by cellular esterases to a non-fluorescent compound, which was later oxidized by the ROS into 2′,7′-dichlorofluorescein (DCF). DCF is a highly fluorescent compound that can be detected by fluorescence spectroscopy with maximum excitation and emission bands at $\lambda=485$ and 520 nm, respectively.

K562 (chronic myelogenous leukemia) cells were cultured in RPMI 1640 medium supplemented with antibiotics and 10% fetal calf serum under a 5% CO_2/95% air atmosphere. Next, 10×10^4 cells per well were stained with 20 μM DCFDA in the culture media and were then incubated for 30 min at 37 °C. After staining, the cells were centrifuged and suspended in complete medium without phenol red, and 10×10^4 cells were seeded on each well of a 96-well plate (PerkinElmer). Next, the cells were incubated for 4 h with the test compounds at concentrations of 5, 10, 20, 50, 100, and 200 μM. Stock solutions of the test compounds were freshly prepared in DMSO. The concentration of DMSO in the cell culture medium was 1%. Cells treated with 50 and 100 μM H_2O_2 served as positive controls. After incubation, fluorescence in each well was measured (excitation at $\lambda=485$ nm, emission measured at $\lambda=520$ nm) by using a microplate reader FLUOStar Omega (BMG-Labtech, Germany). The increase in the fluorescence intensity of DCF was a sign of an increase in ROS levels. For normalization of the data, the DCF fluorescence intensity level in the control cells (exposed to 1% DMSO and 20 μM DCFDA) was taken as 1.0.

Computational Details

Quantum-chemical calculations providing molecular orbitals (HOMO–LUMO), energy-minimized molecular geometries, and vibrational spectra of **10 f** were obtained by using density functional theory (DFT) as implemented in the Gaussian 09 (Revision C.01) program package.[60] We utilized the PBE0 hybrid functional[61] and 6-31G* basis set.[62] Complete ground-state geometry optimization was afforded without symmetry constraints. Only default convergence criteria were used during geometry optimization. Initial atomic coordinates were imported from the crystal structure. Optimized structures in the singlet state were indicated to be local minima (no imaginary frequencies). Selected theoretical and experimental metric parameters are provided in Figure 2. Molecular orbitals were acquired by using Avogadro (an open-source molecular builder and visualization tool, Version 1.1.0).[63]

Acknowledgements

We thank the National Institutes of Health (NIH, CA111329 and F.A.C. for R15GM112395) and the Statutory Funds of CMMS PAS for support of this research. The NSF awards (CHE-0821487, CHE-0722547, and CHE-1048719) and OU Research Excellence Fund are also acknowledged.

Keywords: alkynes · antiproliferative agents · antitumor agents · cobalt · nucleosides

[1] a) P. Herdewijn, *Modified Nucleosides in Biochemistry Biotechnology and Medicine*, Wiley-VCH, Weinheim, **2008**; b) J. P. Godefridus, *Deoxynucleoside Analogs in Cancer Therapy*, Humana Press, Totowa, **2006**; c) P. Merino, *Chemical Synthesis of Nucleoside Analogues*, Wiley, Hoboken, NJ, **2013**.

[2] a) L. P. Jordheim, D. Durantel, F. Zoulim, C. Dumontet, *Nat. Rev. Drug Discovery* **2013**, *12*, 447–464; b) C. M. Galmarini, J. R. Mackey, C. Dumontet, *Lancet Oncol.* **2002**, *3*, 415–424; c) C. M. Galmarini, *Electr. J. Oncol.* **2002**, *1*, 22–32.

[3] Recent representative examples: a) Z. W. Wen, S. H. Suzol, J. F. Peng, Y. Liang, R. Snoeck, G. Andrei, S. Liekens, S. F. Wnuk, *Arch. Pharm.* **2017**, *350*, e1700023; b) H. Amdouni, G. Robert, M. Driowya, N. Furstoss, C. Metier, A. Dubois, M. Dufies, M. Zerhouni, F. Orange, S. Lacas-Gervais, K. Bougrin, A. R. Martin, P. Auberger, R. Benhida, *J. Med. Chem.* **2017**, *60*, 1523–1537; c) V. Alexander, J. Song, J. Yu, J. H. Choi, J.-H. Kim, S. K. Lee, W. J. Choi, L. S. Jeong, *Arch. Pharmacal Res.* **2015**, *38*, 966–972; d) H. V. Nguyen, A. Sallustrau, J. Balzarini, M. R. Bedford, J. C. Eden, N. Georgousi, N. J. Hodges, J. Kedge, Y. Mehellou, C. Tselepis, J. H. R. Tucker, *J. Med. Chem.* **2014**, *57*, 5817–5822.

[4] E. Bobrovnikova-Marjon, J. B. Hurov, *Annu. Rev. Med.* **2014**, *65*, 157–170.

[5] A. R. Kore, I. Charles, *Curr. Org. Chem.* **2012**, *16*, 1996–2013.

[6] a) G. Jaouen, M. Salmain, *Bioorganometallic Chemistry: Applications in Drug Discovery, Biocatalysis, and Imaging*, Wiley-VCH, Weinheim, **2015**, pp. 1–424; b) H. B. Kraatz, N. Metzler-Nolte, *Concepts and Models in Bioinorganic Chemistry*, Wiley-VCH, Weinheim, **2006**, pp. 1–443; c) G. Jaouen, *Bioorganometallic Chemistry*, Wiley-VCH, Weinheim, **2006**, pp. 1–480.

[7] G. Gasser, *Chimia* **2015**, *69*, 442–446.

[8] G. Gasser, I. Ott, N. Metzler-Nolte, *J. Med. Chem.* **2011**, *54*, 3 – 25.
[9] A. R. Timerbaev, C. G. Hartinger, S. S. Aleksenko, B. K. Keppler, *Chem. Rev.* **2006**, *106*, 2224 – 2248.
[10] C. G. Hartinger, N. Metzler-Nolte, P. J. Dyson, *Organometallics* **2012**, *31*, 5677 – 5685.
[11] I. Ott, B. Kircher, R. Dembinski, R. Gust, *Expert Opin. Ther. Pat.* **2008**, *18*, 327 – 336.
[12] N. Metzler-Nolte, *Nachr. Chem.* **2006**, *54*, 966 – 970.
[13] I. Ott, R. Gust, *Arch. Pharm. Chemi Sci. Ed.* **2007**, *340*, 117 – 126.
[14] T. R. Johnson, B. E. Mann, J. E. Clark, R. Foresti, C. J. Green, R. Motterlini, *Angew. Chem. Int. Ed.* **2003**, *42*, 3722 – 3729; *Angew. Chem.* **2003**, *115*, 3850 – 3858.
[15] a) K. S. M. Smalley, R. Contractor, N. K. Haass, A. N. Kulp, G. E. Atilla-Gokcumen, D. S. Williams, H. Bregman, K. T. Flaherty, M. S. Soengas, E. Meggers, M. Herlyn, *Cancer Res.* **2007**, *67*, 209 – 217; b) E. Meggers, *Chem. Commun.* **2009**, 1001 – 1010.
[16] K. Wu, S. Top, E. A. Hillard, G. Jaouen, W. E. Geiger, *Chem. Commun.* **2011**, *47*, 10109 – 10111.
[17] C. Policar, B. J. Waern, M.-A. Plamont, S. Clède, C. Mayet, R. Prazeres, J.-M. Ortega, A. Vessières, A. Dazzi, *Angew. Chem. Int. Ed.* **2011**, *50*, 860 – 864; *Angew. Chem.* **2011**, *123*, 890 – 894.
[18] D. Can, B. Spingler, P. Schmutz, F. Mendes, P. Raposinho, C. Fernandes, F. Carta, A. Innocenti, I. Santos, C. T. Supuran, R. Alberto, *Angew. Chem. Int. Ed.* **2012**, *51*, 3354 – 3357; *Angew. Chem.* **2012**, *124*, 3410 – 3413.
[19] a) M. Patra, G. Gasser, M. Wenzel, K. Merz, J. E. Bandow, N. Metzler-Nolte, *Organometallics* **2012**, *31*, 5760 – 5771; b) M. Wenzel, M. Patra, C. H. R. Sengers, I. Ott, J. J. Stepanek, A. Pinto, P. Prochnow, C. Vuong, S. Langklotz, N. Metzler-Nolte, J. E. Bandow, *ACS Chem. Biol.* **2013**, *8*, 1442 – 1450; c) M. Patra, M. Wenzel, P. Prochnow, V. Pierroz, G. Gasser, J. E. Bandow, N. Metzler-Nolte, *Chem. Sci.* **2015**, *6*, 214 – 224.
[20] D. P. Day, T. Dann, D. L. Hughes, V. S. Oganesyan, D. Steverding, G. G. Wildgoose, *Organometallics* **2014**, *33*, 4687 – 4696.
[21] L. Wei, J. Babich, W. C. Eckelman, J. Zubieta, *Inorg. Chem.* **2005**, *44*, 2198 – 2209.
[22] M. Etheve-Quelquejeu, J.-P. Tranchier, F. Rose-Munch, E. Rose, L. Naesens, E. De Clercq, *Organometallics* **2007**, *26*, 5727 – 5730.
[23] a) C. Hirschhäuser, J. Velcicky, D. Schlawe, E. Heßler, A. Majdalani, J.-M. Neudörfl, A. Prokop, T. Wieder, H.-G. Schmalz, *Chem. Eur. J.* **2013**, *19*, 13017 – 13029; b) D. Schlawe, A. Majdalani, J. Velcicky, E. Heßler, T. Wieder, A. Prokop, H.-G. Schmalz, *Angew. Chem. Int. Ed.* **2004**, *43*, 1731 – 1734; *Angew. Chem.* **2004**, *116*, 1763 – 1766.
[24] C. Prinz, E. Vasyutina, G. Lohmann, A. Schrader, S. Romanski, C. Hirschhäuser, P. Mayer, C. Frias, C. D. Herling, M. Hallek, H.-G. Schmalz, A. Prokop, D. Mougiakakos, M. Herling, *Mol. Cancer* **2015**, *14*, 114.
[25] M. C. Heffern, N. Yamamoto, R. J. Holbrook, A. L. Eckermann, T. J. Meade, *Curr. Opin. Chem. Biol.* **2013**, *17*, 189 – 196.
[26] C. R. Munteanu, K. Suntharalingam, *Dalton Trans.* **2015**, *44*, 13796 – 13808.
[27] a) A. Gross, M. Neukamm, N. Metzler-Nolte, *Dalton Trans.* **2011**, *40*, 1382 – 1386; b) M. A. Neukamm, A. Pinto, N. Metzler-Nolte, *Chem. Commun.* **2008**, 232 – 234; c) G. Gasser, M. A. Neukamm, A. Ewers, O. Brosch, T. Weyhermüller, N. Metzler-Nolte, *Inorg. Chem.* **2009**, *48*, 3157 – 3166.
[28] A. B. J. Withey, G. Chen, T. L. Uyen Nguyen, M. H. Stenzel, *Biomacromolecules* **2009**, *10*, 3215 – 3226.
[29] a) S. Top, H. El Hafa, A. Vessières, M. Huché, J. Vaissermann, G. Jaouen, *Chem. Eur. J.* **2002**, *8*, 5241 – 5249; b) D. Osella, F. Galeotti, G. Cavigiolio, C. Nervi, K. I. Hardcastle, A. Vessières, G. Jaouen, *Helv. Chim. Acta* **2002**, *85*, 2918 – 2925.
[30] A. Nikam, A. Ollivier, M. Rivard, J. L. Wilson, K. Mebarki, T. Martens, J.-L. Dubois-Rande, R. Motterlini, R. Foresti, *J. Med. Chem.* **2016**, *59*, 756 – 762.
[31] a) I. Ott, B. Kircher, R. Gust, *J. Inorg. Biochem.* **2004**, *98*, 485 – 489; b) T. Roth, C. Eckert, H.-H. Fiebig, M. Jung, *Anticancer Res.* **2002**, *22*, 2281 – 2284; c) I. Ott, T. Koch, H. Shorafa, Z. Bai, D. Poeckel, D. Steinhilber, R. Gust, *Org. Biomol. Chem.* **2005**, *3*, 2282 – 2286.
[32] For CO-releasing mechanistic studies and interaction with DMSO, see: A. J. Atkin, S. Williams, P. Sawle, R. Motterlini, J. M. Lynam, I. J. S. Fairlamb, *Dalton Trans.* **2009**, 3653 – 3656.
[33] K. Schmidt, M. Jung, R. Keilitz, B. Schnurr, R. Gust, *Inorg. Chim. Acta* **2000**, *306*, 6 – 16.
[34] I. Ott, R. Gust, *Biometals* **2005**, *18*, 171 – 177.
[35] I. Ott, K. Schmidt, B. Kircher, P. Schumacher, T. Wiglenda, R. Gust, *J. Med. Chem.* **2005**, *48*, 622 – 629.
[36] a) I. Ott, B. Kircher, C. P. Bagowski, D. H. Vlecken, E. B. Ott, J. Will, K. Bensdorf, W. S. Sheldrick, R. Gust, *Angew. Chem. Int. Ed.* **2009**, *48*, 1160 – 1163; *Angew. Chem.* **2009**, *121*, 1180 – 1184; b) G. Rubner, K. Bensdorf, A. Wellner, B. Kircher, S. Bergemann, I. Ott, R. Gust, *J. Med. Chem.* **2010**, *53*, 6889 – 6898.
[37] S. D. Schimler, D. J. Hall, S. L. Debbert, *J. Inorg. Biochem.* **2013**, *119*, 28 – 37.
[38] C. D. Sergeant, I. Ott, A. Sniady, S. Meneni, R. Gust, A. L. Rheingold, R. Dembinski, *Org. Biomol. Chem.* **2008**, *6*, 73 – 80.
[39] S. Meneni, I. Ott, C. D. Sergeant, A. Sniady, R. Gust, R. Dembinski, *Bioorg. Med. Chem.* **2007**, *15*, 3082 – 3088 and references cited therein.
[40] A. Sniady, A. Durham, M. S. Morreale, A. Marcinek, S. Szafert, T. Lis, K. R. Brzezinska, T. Iwasaki, T. Ohshima, K. Mashima, R. Dembinski, *J. Org. Chem.* **2008**, *73*, 5881 – 5889.
[41] M. S. Rao, N. Esho, C. Sergeant, R. Dembinski, *J. Org. Chem.* **2003**, *68*, 6788 – 6790.
[42] A. Sniady, M. D. Sevilla, S. Meneni, T. Lis, S. Szafert, D. Khanduri, J. M. Finke, R. Dembinski, *Chem. Eur. J.* **2009**, *15*, 7569 – 7577.
[43] For alternative protocols for the Sonogashira reaction, see: M. Bakherad, *Appl. Organomet. Chem.* **2013**, *27*, 125 – 140.
[44] For **9 g**, the m.p., UV/Vis data, MS data, elemental analysis, and characteristic ^{1}H NMR signals are described: E. De Clercq, J. Descamps, J. Balzarini, J. Giziewicz, P. J. Barr, M. J. Robins, *J. Med. Chem.* **1983**, *26*, 661 – 666.
[45] Crystals of **10 f** were grown from THF/pentane by diffusion at −20 °C. CCDC 1551456 (**10 f**) contains the supplementary crystallographic data for this paper. These data can be obtained free of charge from The Cambridge Crystallographic Data Centre via http://www.ccdc.cam.ac.uk/data_request/cif.
[46] Related structure **10** with R = 1-cyclohexanol bends in an opposite direction, establishing a contact between the propargyl hydroxy group and the O4 atom of the base (eight-membered ring), O4···H-O9 2.720(5) Å, see Ref. [38].
[47] a) A. Pfletschinger, W. Koch, H.-G. Schmalz, *Chem. Eur. J.* **2001**, *7*, 5325 – 5332; b) J. Overgaard, H. F. Clausen, J. A. Platts, B. B. Iversen, *J. Am. Chem. Soc.* **2008**, *130*, 3834 – 3843.
[48] N. D. de Sousa, R. B. de Lima, A. L. P. Silva, A. A. Tanaka, A. B. F. da Silva, J. D. G. Varela, *Comp. Theor. Chem.* **2015**, *1054*, 93 – 99.
[49] A. L. P. Silva, L. F. de Almeida, A. L. B. Marques, H. R. Costa, A. A. Tanaka, A. B. F. da Silva, J. D. G. Varela, *J. Mol. Model.* **2014**, *20*, 2131.
[50] For an example of induced cleavage of double-stranded DNA, see: S. Bestgen, C. Seidl, T. Wiesner, A. Zimmer, M. Falk, B. Koberle, M. Austeri, J. Paradies, S. Bräse, U. Schepers, P. W. Roesky, *Chem. Eur. J.* **2016**, *23*, 6315 – 6322.
[51] For a recent investigation on dicobalt carbonyl – dppm complexes of natural products, see: A. Moore, J. Ostermann, Y. Ortin, M. J. McGlinchey, *New J. Chem.* **2016**, *40*, 7881 – 7888.
[52] E. Fördős, N. Ungvári, T. Kégl, L. Párkányi, G. Szalontai, F. Ungváry, *Inorg. Chim. Acta* **2008**, *361*, 1832 – 1842.
[53] See for example: a) F.-E. Hong, Y.-L. Huang, H.-L. Chen, *J. Organomet. Chem.* **2004**, *689*, 3449 – 3460; b) W. Y. Man, K. B. Vincent, H. J. Spencer, D. S. Yufit, J. A. K. Howard, P. J. Low, *J. Clust. Sci.* **2012**, *23*, 853 – 872 and references cited therein.
[54] Q. Ma, *Annu. Rev. Pharmacol. Toxicol.* **2013**, *53*, 401 – 426.
[55] H. Pelicano, D. Carney, P. Huang, *Drug Resist. Updates* **2004**, *7*, 97 – 110.
[56] C. Martin-Cordero, A. J. Leon-Gonzalez, J. M. Calderon-Montano, E. Burgos-Moron, M. Lopez-Lazaro, *Curr. Drug Targets* **2012**, *13*, 1006 – 1028.
[57] M. H. Raza, S. Siraj, A. Arshad, U. Waheed, F. Aldakheel, S. Alduraywish, M. Arshad, *J. Cancer Res. Clin. Oncol.* **2017**, *143*, 1789 – 1809.
[58] M. Maszewska, J. Leclaire, M. Cieślak, B. Nawrot, A. Okruszek, A.-M. Caminade, J.-P. Majoral, *Oligonucleotides* **2003**, *13*, 193 – 205.
[59] X. Zhang, Y. Chen, G. Cai, X. Li, D. Wang, *Chem. Biol. Interact.* **2017**, *277*, 91 – 100.
[60] Gaussian 09 (Revision C.01), M. J. Frisch, G. W. Trucks, H. B. Schlegel, G. E. Scuseria, M. A. Robb, J. R. Cheeseman, G. Scalmani, V. Barone, B. Mennucci, G. A. Petersson, H. Nakatsuji, M. Caricato, X. Li, H. P. Hratchian, A. F. Izmaylov, J. Bloino, G. Zheng, J. L. Sonnenberg, M. Hada, M.

Ehara, K. Toyota, R. Fukuda, J. Hasegawa, M. Ishida, T. Nakajima, Y. Honda, O. Kitao, H. Nakai, T. Vreven, J. A. Montgomery, Jr., J. E. Peralta, F. Ogliaro, M. Bearpark, J. J. Heyd, E. Brothers, K. N. Kudin, V. N. Staroverov, T. Keith, R. Kobayashi, J. Normand, K. Raghavachari, A. Rendell, J. C. Burant, S. S. Iyengar, J. Tomasi, M. Cossi, N. Rega, J. M. Millam, M. Klene, J. E. Knox, J. B. Cross, V. Bakken, C. Adamo, J. Jaramillo, R. Gomperts, R. E. Stratmann, O. Yazyev, A. J. Austin, R. Cammi, C. Pomelli, J. W. Ochterski, R. L. Martin, K. Morokuma, V. G. Zakrzewski, G. A. Voth, P. Salvador, J. J. Dannenberg, S. Dapprich, A. D. Daniels, Ö. Farkas, J. B. Foresman, J. V. Ortiz, J. Cioslowski, D. J. Fox, Gaussian, Inc., Wallingford, CT, **2010**.

[61] C. Adamo, V. Barone, *J. Chem. Phys.* **1999**, *110*, 6158 – 6170.

[62] G. A. Petersson, M. A. Al-Laham, *J. Chem. Phys.* **1991**, *94*, 6081 – 6090.

[63] M. Hanwell, D. Curtis, D. Lonie, T. Vandermeersch, E. Zurek, G. Hutchison, *J. Cheminf.* **2012**, *4*, 1 – 17; Avogadro (Version 1.1.0) is available via http://avogadro.openmolecules.net/.

Received: October 27, 2017
Version of record online January 18, 2018

